

# Study of light proton-rich nuclei by complete kinematics measurements<sup>\*</sup>

T. Zerguerras<sup>1</sup>, B. Blank<sup>2,a</sup>, Y. Blumenfeld<sup>1</sup>, T. Suomijärvi<sup>1</sup>, D. Beaulieu<sup>1</sup>, B.A. Brown<sup>3</sup>, M. Chartier<sup>2,b</sup>, M. Fallot<sup>1,c</sup>, J. Giovinazzo<sup>2</sup>, C. Jouanne<sup>4</sup>, V. Lapoux<sup>4</sup>, I. Lhenry-Yvon<sup>1</sup>, W. Mittig<sup>5</sup>, P. Roussel-Chomaz<sup>5</sup>, H. Savajols<sup>5</sup>, J.A. Scarpaci<sup>1</sup>, A. Shrivastava<sup>1,d</sup>, and M. Thoennessen<sup>3</sup>

<sup>1</sup> Institut de Physique Nucléaire, IN2P3-CNRS, F-91406 Orsay, France

<sup>2</sup> CEN Bordeaux-Gradignan, Le Haut-Vigneau, F-33175 Gradignan Cedex, France

<sup>3</sup> NSCL, Michigan State University, East Lansing, MI 48824, USA

<sup>4</sup> CEA Saclay, DSM/DAPNIA/SPhN, F-91191 Gif-sur-Yvette Cedex, France

<sup>5</sup> GANIL, B.P. 5027, F-14076 Caen Cedex 5, France

Received: 30 September 2003 / Revised version: 27 November 2003 /

Published online: 2 June 2004 – © Società Italiana di Fisica / Springer-Verlag 2004

Communicated by D. Guereau

**Abstract.** Light proton-rich bound and unbound nuclei were produced by means of stripping reactions of secondary beams of  $^{20}\text{Mg}$  and  $^{18}\text{Ne}$ . The decays of the unbound nuclei  $^{18,19}\text{Na}$  have been measured by detecting their decay products  $^{17,18}\text{Ne}$  and one proton and by performing an invariant-mass reconstruction. For  $^{18}\text{Na}$ , the present work is the first measurement of its decay. As the decay scheme of this nucleus could not be determined, two possible scenarios are proposed and discussed. In addition, the decay of excited states in  $^{17}\text{Ne}$  via two-proton emission was observed. The proton-proton angular distribution is isotropic for the first two-proton-emitting states, whereas higher-lying states seem to decay by a correlated two-proton emission, consistent with a  $^2\text{He}$  emission pattern for part of the decay strength.

**PACS.** 21.10.-k Properties of nuclei; nuclear energy levels – 23.40.-s  $\beta$  decay; double  $\beta$  decay; electron and muon capture – 23.50.+z Decay by proton emission

## 1 Introduction

Over the last years, nuclear-structure studies have increasingly focused on nuclei far from stability. The proton drip line is relatively easy to reach, and nuclei at and beyond this limit are of great interest, particularly since they may decay by direct two-proton emission [1]. However, nuclei beyond the drip line and excited states of bound nuclei are particle unstable, and their study requires the use of specific techniques. One such method is complete-kinematics measurements, where the nature and the momentum vectors of all the decay products of a given state are detected in coincidence. The total decay energy can then be deduced, and the mass excess of the ground state and of

excited states inferred. In addition, when two-particle decay occurs, energy and angular correlations between these particles can be constructed.

Two-proton emission may be either sequential, occurring through a state of the intermediate nucleus, or simultaneous. In the latter case, one may schematically distinguish  $^2\text{He}$  emission, where the two protons are emitted in the form of a resonance, from uncorrelated “democratic” decay. Experimentally, this distinction can be made through the study of proton angular correlations. Very recently, the first case of ground-state two-proton radioactivity was reported [2,3] for the nucleus  $^{45}\text{Fe}$ . However, no angular correlations could be measured. In the case of unbound states, correlations can be measured when complete-kinematics experiments are performed, thus motivating such studies. In the present experiment, several issues relating to two-proton decay of unbound states were investigated.

The isotope  $^{18}\text{Na}$  may be produced in the decay of the two-proton unbound nucleus  $^{19}\text{Mg}$ , if the decay is sequential and proceeds via an intermediate state. The decay pattern of  $^{19}\text{Mg}$  depends therefore very sensitively on the mass excess of  $^{18}\text{Na}$  and on the question whether the

<sup>\*</sup> Experiment performed at the GANIL facility, Caen, France.

<sup>a</sup> e-mail: blank@cenbg.in2p3.fr

<sup>b</sup> Present address: Physics Department, University of Liverpool, Liverpool, UK.

<sup>c</sup> Present address: SUBATECH, Ecole des Mines, BP 20722, F-44307 Nantes Cedex, France.

<sup>d</sup> Permanent address: Bhabha Atomic Research Center, Mumbai, India.

sequential decay is energetically allowed or not. No mass measurement of  $^{18}\text{Na}$  has yet been reported. In the present experiment, we determined the mass excess of  $^{18}\text{Na}$  from  $^{17}\text{Ne} + p$  events.

In the case of two-proton ( $2p$ ) emission from excited states, *e.g.* after population of highly excited states by  $\beta$ -decay, the de-excitation of these states usually proceeds via a sequential decay, as many intermediate states are energetically available. However, with decreasing excitation energy fewer intermediate states are accessible, in particular as pairing pushes the levels in the two-proton parent nucleus down in energy. Nuclear-structure effects might then in some cases favour a direct two-proton emission, although a sequential decay is energetically possible. In such a direct decay, the two protons might not be emitted isotropically, but rather exhibit a  $^2\text{He}$ -type correlation.

In the present experiment, we studied two-proton emission from excited states in  $^{17}\text{Ne}$  populated in a one-neutron stripping reaction on  $^{18}\text{Ne}$ . By measuring the complete kinematics of the reaction products, two protons and  $^{15}\text{O}$ , we could determine the excitation energy spectrum of  $^{17}\text{Ne}$  and the angle between the two protons in the centre of mass of the decaying system.

## 2 Experimental setup and procedure

The experiment was performed at the Grand Accélérateur National d'Ions Lourds (GANIL, Caen, France) using a primary beam of  $^{24}\text{Mg}^{12+}$  at 95 MeV/nucleon with an intensity of 700 enA on a  $650\text{ mg/cm}^2$  thick  $^{12}\text{C}$  target. The secondary beam was produced by projectile fragmentation in the SISSI solenoids [4] and selected by means of a  $242\text{ mg/cm}^2$  thick plastic degrader located in the dispersive plane of the ALPHA spectrometer. The beam was composed of 11% of  $^{17}\text{F}$  at 33 MeV/nucleon, 87% of  $^{18}\text{Ne}$  at 36 MeV/nucleon, and 2% of  $^{20}\text{Mg}$  at 43 MeV/nucleon, with a total intensity of  $5 \times 10^3$  pps.

The experimental arrangement to study unbound nuclear states is sketched in fig. 1. A  $47\text{ mg/cm}^2$  thick  $^9\text{Be}$  target, located in the centre of the SPEG [5] scattering chamber was used as a secondary reaction target to produce the unbound nuclei. The incoming beam was tracked event by event by two low-pressure multiwire proportional chambers, CATS1 and CATS2 [6], located 1592 and 275 mm upstream from the target, yielding an event-by-event determination of the position and the angle of the beam on target with a resolution of 1 mm and  $0.2^\circ$ , respectively.

Complete-kinematics measurements of outgoing fragments and light charged particles were performed. For the study of  $^{18,19}\text{Na}$ , break-up events of incoming  $^{20}\text{Mg}$  ions were used, whereas  $^{18}\text{Ne}$ -induced events were used for the study of  $2p$  emission from  $^{17}\text{Ne}$ . The beam particle selection was performed by means of the time of flight between a microchannel plate detector, located at the exit of the ALPHA spectrometer, and the CATS2 chamber.

The energy and scattering angle of the recoiling proton were measured using the MUST array [7] which consists of eight telescopes comprising a silicon strip detector backed

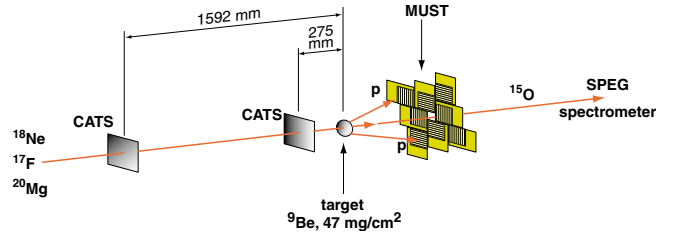


**Fig. 1.** Schematic view of the experimental setup consisting of the CATS tracking chambers, the target, the MUST array, and the SPEG spectrometer.

by a Si(Li) diode and CsI crystals. Each double-sided silicon strip detector ( $60 \times 60\text{ mm}^2$  size,  $300\text{ }\mu\text{m}$  thick with 60 strips 1 mm wide on each side) yields a localisation in both  $X$  and  $Y$  directions with a 1 mm resolution. The MUST telescopes were mounted in the SPEG reaction chamber on a mechanical block located 40 cm downstream from the target and centered at  $0^\circ$  around a  $30\text{ mm} \times 30\text{ mm}$  square hole to allow for the passage of the beam and of the forward-focused heavy fragments. The angular coverage for the proton detection ran between  $2^\circ$  and  $25^\circ$  in the laboratory frame. The angular resolution obtained was  $0.1^\circ$ . The energy range of the protons detected was between 0.8 MeV and 45 MeV due to the 0.8 MeV threshold of the silicon strip detectors, which triggered the electronics. Protons were unambiguously identified by the  $\Delta E$ - $E$  method using energy loss measurements in the silicon strip and the Si(Li) detectors (see fig. 2(a)). The energy calibration of the silicon strip detectors was accomplished using a three-peak  $\alpha$ -particle source containing  $^{233}\text{U}$ ,  $^{239}\text{Pu}$ , and  $^{241}\text{Am}$ . The Si(Li) and CsI detectors were calibrated offline from the known energy loss of protons from the decay of unbound nuclei in the silicon strip detector. These calibrations were checked by measurements where the mount was rotated to large laboratory angles and detected recoiling protons from the elastic and inelastic scattering of the primary  $^{24}\text{Mg}$  beam from a  $\text{CH}_2$  target.

The heavy recoils,  $^{17,18}\text{Ne}$  and  $^{15}\text{O}$ , were detected and analysed in the SPEG spectrometer [5] equipped with a focal-plane detection system including two stripped-cathode drift chambers, a Bragg ionization chamber and a plastic scintillator. Unit mass and charge resolution was obtained by the  $\Delta E$ -TOF method, where the time of flight was measured between the second beam tracking detector CATS2 and the SPEG plastic detector and the energy loss signal was provided by the Bragg chamber (see fig. 2(b)). The focal-plane position, related to the momentum, and the scattering angle of the detected ions were deduced from the positions measured in the two drift chambers. The SPEG spectrometer was centered at  $0^\circ$  covering  $\pm 2^\circ$  in both horizontal and vertical directions and a solid angle of 5 msr. The magnetic rigidity was centered at 1.538 Tm, with a momentum acceptance of  $\pm 3.5\%$ . Angular resolutions obtained in the horizontal and the vertical planes were  $0.06^\circ$  and  $0.4^\circ$ , respectively. The momentum resolution was  $\Delta p/p = 10^{-4}$ .

The invariant masses of different unbound nuclear states were obtained event by event from the total energy

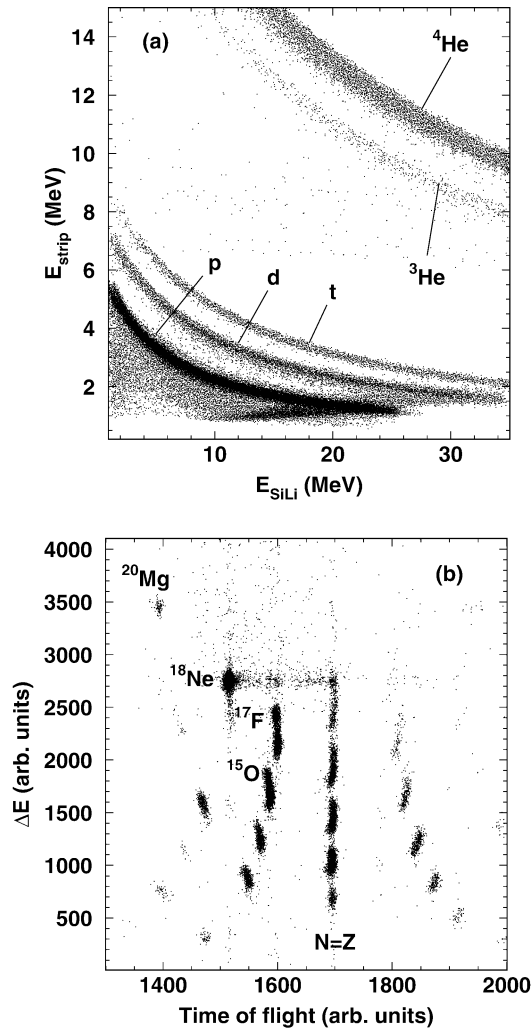


**Fig. 2.** (a) Light-particle identification spectrum from the MUST detector. The energy loss in the silicon strip detectors is plotted as a function of the energy signal from the Si(Li) detectors. Particles between protons and  $^4\text{He}$  are clearly separated. (b) Particle identification spectrum of the energy loss from the SPEG ionisation chamber as well as the time of flight between the CATS2 detector and the SPEG plastic scintillator. The spectrum shows the fragments produced in the secondary beryllium target from the three incoming isotopes  $^{17}\text{F}$ ,  $^{18}\text{Ne}$ , and  $^{20}\text{Mg}$ .

and the momentum for the proton(s) and the heavy recoil. In the spectra, we plot  $\sqrt{(\sum E_i)^2 - (\sum \mathbf{p}_i)^2} - A \times m_u$ , where  $E_i$  and  $\mathbf{p}_i$  are the total energy and the momentum of the different decay products,  $A$  is the mass number of the decaying nucleus and  $m_u$  is the atomic mass unit. This is equal to the mass excess  $\Delta$  of the parent nucleus in the case of a decay to the ground state of the daughter nucleus, hence the labeling  $\Delta$  of the  $x$ -axis in our plots. However, in the absence of  $\gamma$ -ray measurements, we can only conjecture on the final-state energy.

Monte Carlo simulations, taking into account the acceptance of the detection system, the energy loss as well as energy and angular straggling in the target, and the

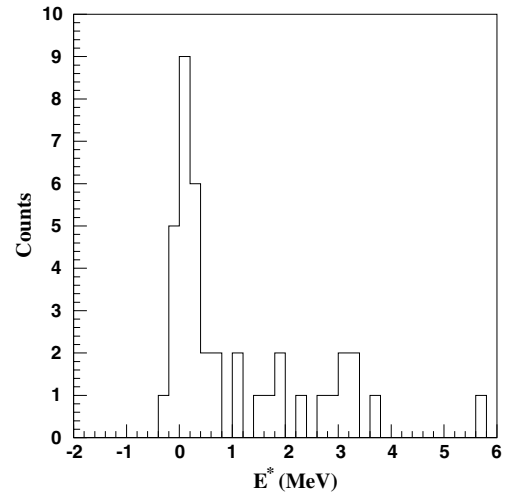


**Fig. 3.** Excitation energy spectrum for  $^{18}\text{Ne} + p$  events. The peak at 0.16(11) MeV (mass excess  $\Delta = 13.09(11)$  MeV) contains events from the ground state as well as from the first excited state at  $E^* = 120$  keV.

energy and angular resolutions of the detectors demonstrated that the acceptance had no influence on the mean value extracted for the invariant mass and yielded an instrumental resolution of  $(250 \pm 50)$  keV. The systematic error was estimated by extracting the proton separation energies of  $^{18}\text{Ne}$  and  $^{17}\text{F}$  from measured  $^{17}\text{F} + p$  and  $^{16}\text{O} + p$  coincidence events. The results obtained agree with the tabulated experimental values [8] to better than 100 keV, and thus in the following 100 keV will be adopted as the systematic error for our invariant-mass measurements. In the case of  $^{18}\text{Na}$ , the ground-state mass excess of  $^{17}\text{Ne}$  is used which has an uncertainty of 50 keV. We therefore adopt a systematic error of 150 keV in this case.

### 3 Experimental results

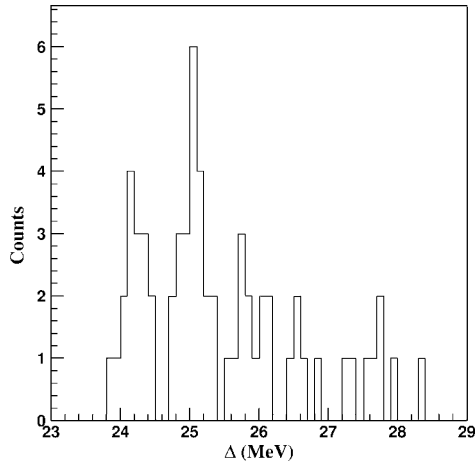
The invariant mass is directly related to the energy available in the decay. If a decay to the ground state of the daughter nucleus is assumed, and the mass excess of this state is known, then the invariant mass can be converted into a mass excess of the decaying state. Moreover, if the mass excess of the ground state of the parent nucleus is known, the mass excess scale can be straightforwardly converted into excitation energy. Since no gamma-ray coincidences were measured in this experiment, we have no experimental determination of the final states populated. This induces uncertainties which will become apparent in the case of  $^{18}\text{Na}$  (see sect. 3.2).

#### 3.1 The case of $^{19}\text{Na}$

Figure 3 displays the excitation energy spectrum as determined from the invariant mass obtained for  $^{19}\text{Na}$  from  $^{18}\text{Ne} + p$  events. We used the mass excess value from Audi

**Table 1.** Mass excess predictions for the ground state of  $^{18}\text{Na}$  are compared to the present experimental result.

Audi & Wapstra [8]	Jänecke & Masson [13]	Pape & Antony [14]	Present result
25.3(4) MeV	25.4(2) MeV	25.7(2) MeV	24.19(16) MeV / 25.04(17) MeV

**Fig. 4.** Invariant-mass spectrum for  $^{17}\text{Ne} + p$  events. Possible explanations for the peaks at 24.19 MeV and at 25.04 MeV as decays from states in  $^{18}\text{Na}$  to states of  $^{17}\text{Ne}$  are given in the text.

*et al.* [8] for  $^{19}\text{Na}$  to determine the excitation energy. The figure shows a pronounced peak at 0.16(11) MeV. We interpret this peak as originating from the decay of the  $^{19}\text{Na}$  ground and first excited states, which, due to their small energy difference of only 120 keV, are not resolved in our experiment, to the ground state of  $^{18}\text{Ne}$ . The peak position close to zero excitation energy shows the good agreement with two previous measurements of the ground-state mass excess of  $^{19}\text{Na}$  which yielded values of 12.97(7) MeV [9] and 12.93(1) MeV [10]. The slight shift to higher energies in the present result can be explained by the contribution of ground-state and excited-state events. This shows again that the systematic error in our analysis is less than 100 keV, as mentioned above. New results for higher-lying states of  $^{19}\text{Na}$  have also been obtained recently [11,12]. However, as they cover different states as compared to our present results, a direct comparison is not possible.

### 3.2 The mass excess and the decay of $^{18}\text{Na}$

To construct the invariant-mass spectrum of  $^{18}\text{Na}$ ,  $^{17}\text{Ne} + p$  events were analysed. The result is shown in fig. 4. A two-peak structure is clearly visible with mass excess values of 24.19(16) MeV and 25.04(17) MeV. The widths are 0.34(9) MeV and 0.54(13) MeV, respectively. Corrected for an experimental resolution of 250(50) keV, this yields widths of 230(100) keV and 480(140) keV for the two states. In table 1, we give values for ground-state

mass excess predictions from Audi and Wapstra [8], from Jänecke and Masson using the Garvey and Kelson relation [13], as well as from Pape and Antony [14]. In the following, we will present two different interpretations of our data: i) assuming that the low-energy peak in fig. 4 is due to a ground-state-to-ground-state decay which implies a very large Thomas-Ehrman shift [15] and ii) assuming that the lowest peak is due to an excited-state-to-excited-state decay and the second peak is the ground-state-to-ground-state decay which is in disagreement with theoretical expectations.

A first possibility is that the 24.19 MeV peak is due to the decay of the  $^{18}\text{Na}$  ground state to the ground state of  $^{17}\text{Ne}$ , whereas the 25.04 MeV peak originates from the decay of the first excited state in  $^{18}\text{Na}$  to the ground state of  $^{17}\text{Ne}$ . A comparison with the theoretical mass predictions (see table 1) shows that such a scenario implies a strong Thomas-Ehrman shift [15]. Such a scenario yields a proton decay  $Q$  value  $Q_p = 0.42(17)$  MeV, where we have taken the  $^{17}\text{Ne}$  mass excess from ref. [8]. For such a relatively low  $Q$  value, a Thomas-Ehrman shift of more than 1 MeV is unexpected, but cannot be completely ruled out. From the systematics in ref. [15], one would expect a value of the order of 0.5 MeV.

Another interpretation of the peak at 24.19 MeV is the decay of a state in  $^{18}\text{Na}$  to the first excited state in  $^{17}\text{Ne}$  at 1.288(8) MeV [16]. The decaying state could be the ground state or a low-lying first excited state. However, the energy difference between the peaks at 24.19 MeV and at 25.04 MeV is smaller than the excitation energy of the first excited state in  $^{17}\text{Ne}$ . Therefore, a consistent picture for such a scenario arises only if one assumes that the ground state in  $^{18}\text{Na}$  decays to the ground state of  $^{17}\text{Ne}$  and the first excited state of  $^{18}\text{Na}$  decays to the first excited state of  $^{17}\text{Ne}$ . Then the 25.04 MeV peak is due to the ground-state-to-ground-state decay, whereas the 24.19 MeV peak results from the connection of the two first excited states. Such a scenario places the first excited state of  $^{18}\text{Na}$  at  $E^* = 0.44(8)$  MeV.

For these two scenarios, we investigate now which spin/parity for the states involved are most likely and what decay widths we expect from theoretical calculations. In the mirror nucleus,  $^{18}\text{N}$ , the first excited state has  $I^\pi = 2^-$  with an excitation energy  $E^* = 120$  keV, whereas the ground state has  $I^\pi = 1^-$ . Therefore, the ground state of  $^{18}\text{Na}$  and the first excited state are expected to have spin/parity  $I^\pi = 1^-$  and  $I^\pi = 2^-$ , respectively, or vice versa.

**Table 2.** Shell model spectroscopic factors for the decay of states in  $^{18}\text{Na}$  to the ground ( $1/2^-$ ) and first excited ( $3/2^-$ ) state of  $^{17}\text{Ne}$ . The decay of the  $1^-$  state to the  $3/2^-$  state as well as the decay of the  $2^-$  state to the  $1/2^-$  state are clearly favoured based on spectroscopic factors alone (see text).

$^{18}\text{Na}$ state	$^{17}\text{Ne}$ state	Proton orbitals			
		$1s_{1/2}$	$1d_{5/2}$	$1d_{3/2}$	$2s_{1/2}$
$1^-$	$3/2^-$	0.000	0.655	0.017	0.195
$1^-$	$1/2^-$	0.000	–	0.012	0.005
$2^-$	$3/2^-$	0.000	0.182	0.026	0.033
$2^-$	$1/2^-$	–	0.700	0.000	–

Shell model calculations predict that the main components of the states of interest are the following:

$$\begin{aligned}
 ^{18}\text{Na} \quad 1^- & \quad ([\pi(d_{5/2})^3]_{3/2+}[\nu p_{1/2}]) \text{ and} \\
 & \quad ([\pi(d_{5/2})^2]_{2+}[\pi s_{1/2}][\nu p_{1/2}]), \\
 ^{18}\text{Na} \quad 2^- & \quad ([\pi(d_{5/2})^3]_{5/2+}[\nu p_{1/2}]) \text{ and} \\
 & \quad ([\pi(d_{5/2})^2]_{2+}[\pi s_{1/2}][\nu p_{1/2}]), \\
 ^{17}\text{Ne} \quad 1/2^- & \quad ([\pi(d_{5/2})^2]_{0+}[\nu p_{1/2}]), \\
 ^{17}\text{Ne} \quad 3/2^- & \quad ([\pi(d_{5/2})^2]_{2+}[\nu p_{1/2}]).
 \end{aligned}$$

The  $[\pi(d_{5/2})^3]_{3/2+}$  configuration in  $^{18}\text{Na}$  can only connect to the  $[\pi(d_{5/2})^2]_{2+}$  configuration, and thus with these main components the  $1^-$  state can only go to the  $3/2^-$  excited state of  $^{17}\text{Ne}$ . The  $[\pi(d_{5/2})^3]_{5/2+}$  configuration in turn can only decay to the  $[\pi(d_{5/2})^2]_{0+}$  configuration which links thus for the main wave function components the  $2^-$  state to the  $1/2^-$  state. The spectroscopic factors obtained with the *full p-sd* wave functions are given in table 2. The spectroscopic factors associated with the decay of the  $1^-$  state in  $^{18}\text{Na}$  to the  $1/2^-$  state in  $^{17}\text{Ne}$  are indeed small, but not zero. The same is true for the spectroscopic factors for the decay of the  $2^-$  state to the  $3/2^-$  state.

We have used the scattering phase shifts obtained with a Woods-Saxon potential to estimate the decay widths of the  $1^-$  and  $2^-$  states to the states in  $^{17}\text{Ne}$ . In our first scenario, we obtain the following decay widths:

- For the  $1^-$  state as the ground state, the single-particle width for the  $1^-$ -to- $1/2^- s_{1/2}$  decay with  $Q = 0.42$  MeV is about 1.0 keV, and the single-particle decay width for the  $2^-$ -to- $1/2^- s_{1/2}$  decay with  $Q = 1.27$  MeV is 7.1 keV. Together with the spectroscopic factors of 0.005 and 0.70, the decay widths are 0.005 keV and 5.0 keV for the decay of the  $1^-$  and  $2^-$  states to the  $^{17}\text{Ne}$   $1/2^-$  ground state, respectively.
- For the  $2^-$  state as the ground state, the single-particle width for the decay to the  $1/2^-$  state with  $Q = 0.42$  MeV is about 5 eV, and the single-particle decay width for the decay of the  $1^-$  excited state to the  $1/2^-$  ground state with  $Q = 1.27$  MeV is 210 keV. With the spectroscopic factors of 0.70 and 0.005, the

decay widths are 3.5 eV and 1.0 keV for the  $2^-$  and  $1^-$  states, respectively.

With the experimental information obtained in the present work, we are not able to distinguish between these two possibilities. As the first scenario implies a rather large Thomas-Ehrman effect, we do not think that one can simply assume that the level sequence is the same as in the mirror nucleus. More detailed experimental data as well as theoretical calculations are needed to decide which of the two states would be the excited state.

In our second scenario, we assume that the ground state of  $^{18}\text{Na}$  decays to the ground state of  $^{17}\text{Ne}$  and the first excited state decays to the first excited state of  $^{17}\text{Ne}$ . In this case, the excited-state-to-excited-state decay has a  $Q$  value of 1.71 MeV and the ground-state-to-ground-state decay a  $Q$  value of 0.42 MeV. Then the following possibilities arise:

- For the  $1^-$  state, the single-particle width for the  $1^-$  to  $1/2^- s_{1/2}$  decay with  $Q = 1.71$  MeV is about 480 keV, and the single-particle decay width for the  $1^-$  to  $3/2^- s_{1/2}$  decay with  $Q = 0.42$  MeV is about 1.0 keV. Together with the spectroscopic factors of 0.005 and 0.195, the decay widths are 2.4 keV and 0.2 keV to the  $1/2^-$  and  $3/2^-$  states, respectively. Thus, the  $1^-$  state decay should be dominated by the decay to the  $1/2^-$  ground state of  $^{17}\text{Ne}$  unless the  $s_{1/2}$  spectroscopic factor is at least 10 times smaller than its already small theoretical value.
- For the  $2^-$  state, the single-particle width for the decay to the  $1/2^-$  state with  $Q = 1.71$  MeV is 29 keV, and the single-particle decay width for the decay to the  $3/2^-$  state with  $Q = 0.42$  MeV is 1.0 keV. With the spectroscopic factors of 0.70 and 0.033, the decay widths are 20 keV and 0.033 keV to the  $1/2^-$  and  $3/2^-$  states, respectively. Therefore, as for the  $1^-$  state, the decay of the  $2^-$  state to the  $1/2^-$  ground state is strongly favoured.

Therefore, in this second scenario, the excited state of  $^{18}\text{Na}$  is in any case expected to decay to the ground state of  $^{17}\text{Ne}$ , which is in contradiction with our assumption of an excited-state-to-excited-state decay.

If we exclude, based on the theoretical calculations just exposed, a decay of any state in  $^{18}\text{Na}$  to the first excited state in  $^{17}\text{Ne}$ , the low-energy peak in fig. 4 yields the ground-state mass excess of  $^{18}\text{Na}$ . However, as mentioned above, the value thus deduced of  $\Delta = 24.19(16)$  MeV is far lower than any prediction (see table 2). We favour the scenario determined from experiment only where the 25.04(17) MeV peak constitutes the ground-state-to-ground-state decay, whereas the 24.19(16) MeV peak corresponds to the decay of an excited state in  $^{18}\text{Na}$  to the first excited state in  $^{17}\text{Ne}$ . However, before such a decay scheme can be really established, new experimental data are clearly needed.

Depending on the scenario adopted, the  $^{18}\text{Na}$  ground-state mass excess is therefore 25.04(17) MeV or 24.19(16) MeV which includes the 150 keV systematic uncertainty. The first value is in reasonable agreement with

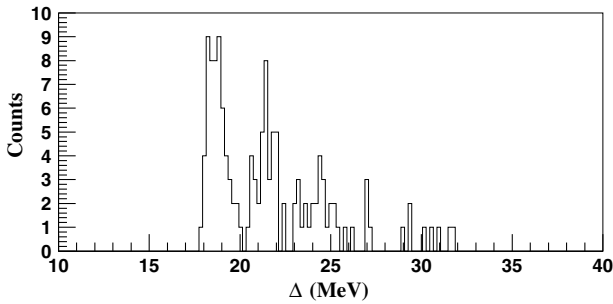


**Fig. 5.** Invariant-mass spectrum for  $^{15}\text{O} + 2\text{p}$  events. The peak at 18.5 MeV is interpreted as the decay of the second and third excited states of  $^{17}\text{Ne}$  by two-proton emission, whereas the activity above 20 MeV arises from the decay of higher-lying states.

the Audi and Wapstra [8] as well as with the Jänecke and Masson [13] predictions. The Pape and Antony prediction [14] would be slightly too high. The second value is much lower than any prediction and would have to be interpreted in terms of a significant Thomas-Ehrman shift [15].

Both mass excess values place the  $^{18}\text{Na} + \text{p}$  mass excess above the  $^{19}\text{Mg}$  mass excess prediction ( $\Delta(^{19}\text{Mg}) = 31.95(30)$  MeV) of Audi and Wapstra. This would tend to favour a direct  $2\text{p}$  decay of  $^{19}\text{Mg}$ . However, the uncertainty and the width may add up to open the sequential channel. In any case, it seems to be interesting to study the decay of this  $2\text{p}$  candidate.

### 3.3 Two-proton emission from $^{17}\text{Ne}$

The decay of excited states in  $^{17}\text{Ne}$  has been studied by analysing events where two protons were observed in coincidence with a  $^{15}\text{O}$  heavy recoil. The invariant-mass spectrum for these events is shown in fig. 5. The pronounced peak at about 18.5 MeV is due to the decay of the second and third excited states in  $^{17}\text{Ne}$  by two-proton emission, whereas the activity above 20 MeV arises from the decay of higher-lying states. The absence of activity below the first peak at 18.5 MeV demonstrates that the first excited state in  $^{17}\text{Ne}$ , although two-proton unbound, does not decay by  $2\text{p}$  emission, in agreement with a recent result from Chromik and co-workers [17].

The measurement of the complete kinematics of the decay products allows us also to determine the angle between the two protons in the centre of mass. This spectrum is shown in fig. 6. The spectrum shows an isotropic distribution with, however, an excess of counts at about  $50^\circ$  in the centre of mass. The Monte Carlo simulations mentioned above, which include experimental acceptances, were used to simulate spectra expected for sequential or uncorrelated three-body decay, *i.e.* a decay to the whole phase space volume, (the shape for these two decay modes is the same, namely isotropic) as well as for a  $^2\text{He}$  decay pattern with a  $^2\text{He}$  resonance energy of about 50 keV. For the sequential decay we do not take into account a possible polarisation of the nucleus after a first proton emission.

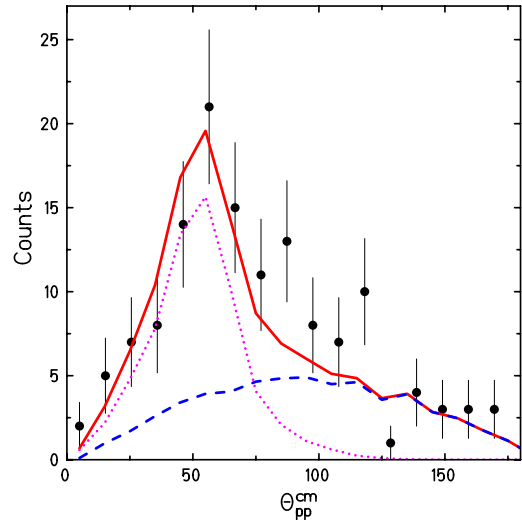


**Fig. 6.** Angular distribution in the centre of mass for all  $2\text{p}$  events correlated with the observation of a  $^{15}\text{O}$  recoil. The dotted curve is a simulation of a correlated two-proton emission via a  $^2\text{He}$  resonance, whereas the dashed line corresponds to a sequential-emission pattern via the ground state of  $^{16}\text{F}$ . The full line is a fit with a 47% sequential and a 53%  $^2\text{He}$  contribution.

These simulations use  $R$ -matrix theory to describe the respective decays. The sequential decay is modelled as a decay through an intermediate state, which is the ground state of  $^{16}\text{F}$ . The  $^2\text{He}$  emission simulations use the proton-proton final-state interaction model of Watson and Migdal [18]. This model together with barrier penetration calculations yields a most probable resonance energy for the two protons of about 50 keV. This resonance energy determines how pronounced the proton-proton angular correlation will be. Lower resonance energies give a more pronounced peak structure for the  $^2\text{He}$  decay pattern, whereas higher resonance energies wash the peak out more and more on approaching an isotropic distribution. Further details of the physics used are described in [19].

A more refined model based on  $R$ -matrix theory was recently proposed by Barker [20,21]. However, the angular distribution of the two protons is not believed to change significantly. This distribution is mainly determined by the effective  $^2\text{He}$  resonance energy which is determined, as mentioned above, by the proton-proton final-state interaction and barrier penetration.

Neither of the two calculations presented in fig. 6 is in agreement with the experimental data. The experimental spectrum is best reproduced with a  $(47 \pm 8)\%$  contribution for sequential decay and a  $(53 \pm 8)\%$  contribution in the  $^2\text{He}$  picture (see fig. 6). Such a fit yields a reduced  $\chi^2$  of 1.28, whereas the fits with only one component increase the reduced  $\chi^2$  by about a factor of 2.6 in both cases.

A more refined comparison can be done by performing energy cuts before projecting the proton-proton angular correlation. For this purpose, we show in fig. 7(a) the spectrum obtained for events with a mass excess corresponding to the 18.5 MeV peak as well as for events above 20.2 MeV

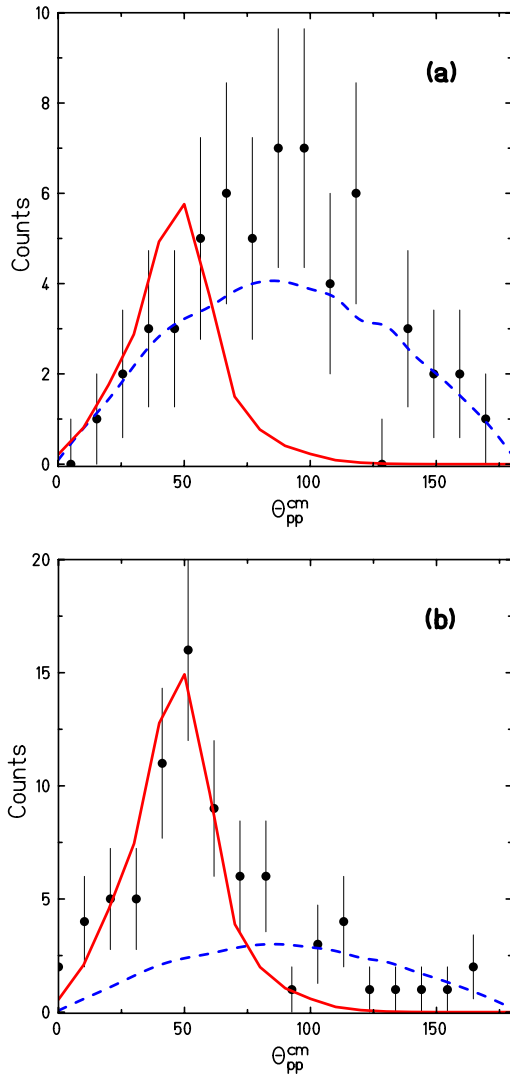


**Fig. 7.** Proton-proton angular distribution for 2p events with a  ${}^{15}\text{O}$  recoil yielding a mass excess of less than 20.2 MeV (a) and above 20.2 MeV (b). The solid and the dashed curves are simulation of a correlated two-proton emission via a  ${}^2\text{He}$  resonance and a sequential-emission pattern, respectively.

of mass excess (fig. 7(b)). Within the limited statistics, the two spectra appear to be different. The spectrum due to the decay of the lower excited states is in agreement with an uncorrelated, isotropic decay, whereas for the spectrum from higher excited states the angular correlation already visible in the spectrum of fig. 6 is even more pronounced. Our fit yields a  $(28 \pm 9)\%$  sequential and a  $(72 \pm 12)\%$   ${}^2\text{He}$  contribution for this high-energy cut with a reduced  $\chi^2 = 0.7$ . The reduced  $\chi^2$  increases by factors of 2 (only  ${}^2\text{He}$  contribution) and 4 (sequential contribution), when a fit with only one component is tried. The low-energy cut, however, is in nice agreement with the sequential component only ( $\chi^2 = 1.0$ ). An attempt to fit the spectrum in fig. 7(a) with a  ${}^2\text{He}$  component alone increases the reduced  $\chi^2$  by a factor of more than 2.

The shape of the spectrum in fig. 7(a) is in agreement with the results from Chromik *et al.* [17] who observed an

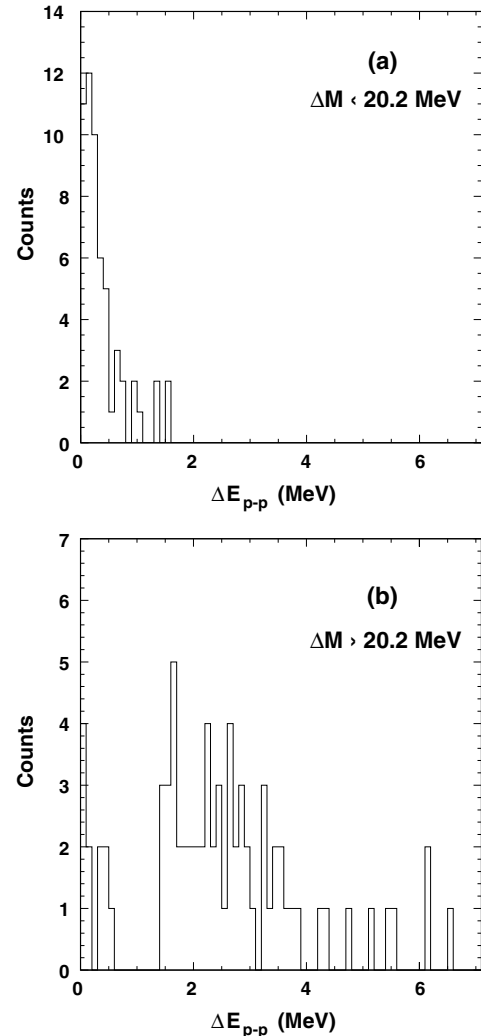


**Fig. 8.** Proton-proton energy difference in the centre of mass for 2p events with a  ${}^{15}\text{O}$  recoil yielding a mass excess of less than 20.2 MeV (a) and above 20.2 MeV (b).

isotropic distribution for the two protons from the second and third excited states in  ${}^{17}\text{Ne}$ . However, in their experiment which used Coulomb excitation to populate excited states in  ${}^{17}\text{Ne}$ , no states above  $E^* = 2$  MeV were populated. The present experimental result seems to suggest that one or several states above  $E^* = 2$  MeV might decay by a correlated two-proton emission.

Additional experimental information can be gained from the energy difference of the two protons emitted in the decay. The result of such an analysis in the centre-of-mass frame of the decaying system is shown in fig. 8 for the two mass excess regions below and above 20.2 MeV. The low-energy part indicates a more or less equal energy sharing between the two protons. This is expected as the intermediate state, the ground state of  ${}^{16}\text{F}$ , is situated roughly half-way between the initial and the final state. The energy difference for the high-energy part shows a few counts close to zero corresponding to similar proton energies and a broad distribution with a significant energy difference between the two protons.

A possible explanation for the observed proton-proton angular correlation and the proton energy difference spectrum could be that the wave function of the highly excited decaying state(s) has only very little overlap with the wave function of energetically accessible states in the one-proton daughter  $^{16}\text{F}$  and thus this or these state(s) decay(s) directly to the ground state of  $^{15}\text{O}$ . Such a picture could arise, if one or several  $^{17}\text{Ne}$  states were two-proton halo states. In this case, a spectroscopic factor close to unity is expected for the decay to the  $^{15}\text{O}$  states. Such a picture is supported by a recent measurement of two-proton removal from  $^{17}\text{Ne}$  at RIKEN [22]. The authors of this paper conclude that the narrow momentum distribution, after two-proton removal, of the  $^{15}\text{O}$  fragments as well as the reaction cross-sections are consistent with a two-proton halo of  $^{17}\text{Ne}$ . Their conclusion is only valid for the ground state of  $^{17}\text{Ne}$ . However, for excited states such a halo effect should be even more pronounced as long as the two weakly bound protons still significantly occupy low- $l$  orbitals. If such a decay occurs by forming a  $^2\text{He}$  resonance, one would, at least in a naive picture, expect that the two protons share their energy equally. However, it might well be that this is only the case of part of the decay strength (counts close to zero in fig. 8(b)), whereas these states decay mainly by a simultaneous decay without any particular p-p correlation and the forward focusing in the angular distribution is mainly due to the final-state interaction of the two simultaneously emitted protons.

To study such decays in more detail and to answer the question whether there is a correlation between the protons beyond final-state interactions, which should be present for any simultaneous two-proton emission, much higher-statistics data, preferentially with better energy resolution, are needed. From the theoretical side, a detailed study of the  $^{17}\text{Ne}$  ground and excited states in terms of their halo structure would help to interpret our data.

It would also be interesting to use the three-body model recently developed by Grigorenko *et al.* (see, *e.g.*, [23]). In this work, realistic proton-proton and proton-nucleus interactions are used to treat two-proton emission as a three-particle decay. These calculations yielded a detailed description of the decay process for  $^{12}\text{O}$  and for  $^{16}\text{Ne}$ . However, an application of this model to excited states of  $^{17}\text{Ne}$  is beyond the scope of the present paper.

## 4 Summary

We have performed complete-kinematics measurements to study the structure of light nuclei beyond the proton drip line. The measurement of the momentum vectors of all decay particles allowed to investigate the ground-state mass excess of  $^{18,19}\text{Na}$  as well as to study two-proton emission from excited states of  $^{17}\text{Ne}$ .

For the decay of  $^{18}\text{Na}$ , two possible schemes were discussed, one which assumes a decay of the ground and first excited state of this nucleus to the ground state of  $^{17}\text{Ne}$  and a second where the first excited state of  $^{18}\text{Na}$  decays to the first excited state of  $^{17}\text{Ne}$ . The first scenario yields a ground-state mass excess of 24.19(16) MeV for  $^{18}\text{Na}$

implying a rather strong Thomas-Ehrman shift, whereas the second scenario yields 25.04(17) MeV, in reasonable agreement with most mass predictions. However, although experimentally plausible, this second decay scheme could not be reproduced by our theoretical calculations. The use of  $\gamma$ -ray detectors in a future experiment should help to clarify the question whether the first excited state of  $^{18}\text{Na}$  decays indeed to the first excited state of  $^{17}\text{Ne}$  or rather to its ground state.

The decay of excited states in  $^{17}\text{Ne}$  by two-proton emission seems to indicate that one or several states with an excitation energy above 2 MeV might decay by a correlated two-proton emission via a  $^2\text{He}$  resonance. However, further experiments are clearly needed to confirm this finding. New experiments to test this hypothesis can take advantage of the high  $^{17,18}\text{Ne}$  beam intensities now available at the SPIRAL facility of GANIL.

We thank P. Gangnant, J.F. Libin, and L. Petizon for their help in setting up the experiment. We are indebted to J.F. Clavelin and the GIP/GANIL group for ensuring the compatibility between the electronics of MUST and the GANIL data acquisition system. This work was supported in part by the Région Aquitaine and by the National Science Foundation under grant No. PHY95-28844.

## References

1. P. Woods, C. Davids, *Annu. Rev. Nucl. Part. Sci.* **47**, 541 (1997).
2. J. Giovinazzo *et al.*, *Phys. Rev. Lett.* **89**, 102501 (2002).
3. M. Pfützner *et al.*, *Eur. Phys. J. A* **14**, 279 (2002).
4. A. Joubert *et al.*, *Proceedings of the Second Conference of the IEEE Particle Accelerator, San Francisco, May 1991*, p. 594.
5. L. Bianchi *et al.*, *Nucl. Instrum. Methods A* **276**, 509 (1989).
6. S. Ottini-Hustache *et al.*, *Nucl. Instrum. Methods A* **431**, 476 (1999).
7. Y. Blumenfeld *et al.*, *Nucl. Instrum. Methods A* **421**, 471 (1999).
8. G. Audi, A.H. Wapstra, *Nucl. Phys. A* **595**, 409 (1995).
9. J. Cerny *et al.*, *Phys. Rev. Lett.* **22**, 612 (1969).
10. W. Benenson *et al.*, *Phys. Lett. B* **58**, 46 (1975).
11. C. Angulo *et al.*, *Phys. Rev. C* **67**, 014308 (2003).
12. F. de Oliveira Santos, to be published in *Proceedings of the International Symposium on Proton-emitting Nuclei PROCON03, Legnaro*, edited by E. Maglione, L. Ferreira.
13. J. Jänecke, P. Masson, *At. Data Nucl. Data Tables* **39**, 265 (1988).
14. A. Pape, M. Antony, *At. Data Nucl. Data Tables* **39**, 201 (1988).
15. E. Comay, I. Kelson, A. Zidon, *Phys. Lett. B* **210**, 31 (1988).
16. V. Guimaraes *et al.*, *Phys. Rev. C* **58**, 116 (1998).
17. M. Chromik *et al.*, *Phys. Rev. C* **66**, 024313 (2002).
18. M. Bernstein, W. Friedman, W. Lynch, *Phys. Rev. C* **29**, 132 (1984).
19. R.A. Kryger *et al.*, *Phys. Rev. Lett.* **74**, 860 (1995).
20. F.C. Barker, *Phys. Rev. C* **59**, 535 (1999).
21. F.C. Barker, *Phys. Rev. C* **63**, 047303 (2001).
22. R. Kanungo *et al.*, *Phys. Lett. B* **571**, 21 (2003).
23. L. Grigorenko *et al.*, *Phys. Rev. C* **64**, 054001 (2001).